Influence of the incident radiation on the energy performance of two small-scale solar Organic Rankine Cycle trigenerative systems: A simulation analysis

Mauro Villarini[a,*], Roberto Tascioni[b,d], Alessia Arteconi[c,d], Luca Cioccolanti[d]

[a] Department of Agriculture and Forest Sciences, Tuscia University of Viterbo, Via San Camillo de Lellis, 01100 Viterbo, Italy
[b] Department DIAEE, Sapienza University of Rome, Via Eudossiana 18, Rome, Italy
[c] Department of Industrial Engineering and Mathematical Sciences, Polytechnic University of Marche, Via Brecce Bianche, 60131 Ancona, Italy
[d] Università Telematica e-Campus, Via Isimbardi 10, 22060 Novedrate, CO, Italy

HIGHLIGHTS

- Two innovative small-scale CCHP solar ORC systems are modelled in TRNSYS/MATLAB.
- The two systems are powered by two different CSP technologies: CPC and LFR.
- The performance is analysed varying location and composition of global irradiance.
- The DNI/GHI ratio has an influence on the system performance.
- Useful hints for the selection of the best CSP technology with DNI are provided.

ARTICLE INFO

ABSTRACT

In this paper, two innovative small-scale solar Organic Rankine Cycle (ORC) trigeneration plants are investigated and compared using a simulation analysis. In particular, the first plant (Plant 1) consists of a 146 m^2 Compound Parabolic Collectors (CPC) solar field, a 3 m^3 diathermic oil storage tank, a 3.5 kWe ORC plant and a 17 kWc absorption chiller, while the second plant (Plant 2) consists of a Linear Fresnel Reflectors (LFR) solar field of equal reflecting area, a phase change material storage tank equipped with reversible heat pipes, a 3.2 kWe ORC unit and the same 17 kWc absorption chiller as the former.

The dynamic performance of the considered plants has been assessed for two Italian locations representative of the European Mediterranean area, Napoli and Messina, having a similar global radiation but a significantly different ratio of direct normal irradiance to diffuse irradiance. The comparison between the two different solar ORC trigeneration systems has revealed the great influence of the solar radiation on the effectiveness of such systems even for locations at similar latitudes. The energy production has been analysed both on a monthly and daily basis. Results have shown that while the performance of Plant 1 is not so sensitive to location and radiation conditions, Plant 2 is greatly affected by these parameters. Moreover, the higher condensing temperatures necessary in summer to supply the absorption chiller significantly limit the electrical efficiency of the solar CPC ORC. On the contrary, the LFR technology allows the achievement of higher temperatures and conversion efficiencies in summer, thus resulting especially suitable for solar cooling applications. In conclusion, this study has highlighted the importance of adequate technology selection with different radiation conditions in order to better exploit the potential of trigenerative solar ORC systems.

1. Introduction

Use of locally available renewable sources all over the world is becoming of paramount importance to guarantee a sustainable development and assure the security of energy supply. Among them, solar energy is one of the most promising as addressed by Pietzcker et al. [1]

Nomenclature

A	area of the collector [m^2]
a_0	first order efficiency coefficient [$W/m^2 \cdot K$]
a_1	second order efficiency coefficient [$W/m^2 \cdot K$]
CCHP	Combined Cooling, Heating and Power
COP	Coefficient Of Performance
CPC	Compound Parabolic Collector
CSP	Concentrated Solar Power
DHI	Diffuse Horizontal Irradiance [W/m^2]
DNI	Direct Normal Irradiation [W/m^2]
ETC	Evacuated Tube Collector
G_b	direct radiation on collector plane [W/m^2]
G_d	diffuse radiation on collector plane [W/m^2]
h_{abs}	operating hours of the absorption chiller [h]
h_{ORC}	operating hours of the ORC unit [h]
HSW	hot sanitary water
HTT	High Temperature storage Tank
IAM	Incident Angle Modifier
LCOE	Levelized Cost Of Energy
LFR	Linear Fresnel Reflector
LTT	Low Temperature storage Tank
NZEB	Nearly Zero Energy Buildings
K_θ	Incident Angle Modifier for direct radiation
K_d	Incident Angle Modifier for diffuse radiation
$\dot{m}_c$	mass flow rate of the cooling water [kg/s]
$\dot{m}_f$	mass flow rate of the organic fluid [kg/s]
NTU	Number of Transfer Units
OM	Operation Mode of Plant 2
P1	Plant n.1
P2	Plant n.2
P_e	Electrical Power [kWe]
P_c	Cooling Power [kWc]
P_t	Thermal Power [kWt]
P_{abs}	cooling power output from the absorption chiller [kW_c]
$P_{abs,in}$	thermal power input to the absorption chiller [kW_t]
$P_{ORC,el}$	electrical power produced by the ORC unit [kW_e]
$P_{ORC,out}$	outlet thermal power from the ORC unit [kW_t]
$P_{ORC,in}$	inlet thermal power to the ORC unit [kW_t]
$P_{SF,in}$	inlet power to the solar field [kW]
$P_{SF,out}$	outlet thermal power from the solar field [kW_t]
PCM	Phase Change Material
PTC	Parabolic Trough Collector
Q_{loss}	heat losses at the receiver [kW_t]
Q_{PCM}	heat exchanged by the PCM [kW_t]

R_{irr}	ratio between DNI to diffuse irradiance
SM	Solar Multiple
TES	Thermal Energy Storage
T_a	ambient air temperature [°C]
T_{av}	average temperature [°C]
T_{in}	inlet temperature of the cooling water at the condenser [°C]
T_m	mean temperature of the fluid in the collector [°C]
T_{out}	outlet temperature of the cooling water at the condenser [°C]
$T_{ORC,off}$	lower bound temperature set-point of the TES [°C]
$T_{ORC,on}$	upper bound temperature set-point of the TES [°C]
$T_{TES,av}$	average temperature of the TES [°C]
Δh_e	actual specific enthalpy difference across the expander [kJ/(kg K)]
Δh_p	actual specific enthalpy difference across the pump [kJ/(kg K)]
ΔT_h	hot period working temperature range of HTT-ORC inlet [°C]
ΔT_c	cold period working temperature range of HTT-ORC inlet [°C]
ΔT_m	mid seasons working temperature range of HTT-ORC inlet [°C]
ΔT_{PCM}	temperature difference between the PCM and the heat transfer medium [°C]
$\Delta t_{int\text{-}timestep}$	time interval of the internal time step [s]

Greek symbols

α	solar elevation angle
β	absorptance coefficient
ε	emittance coefficient
η_{el}	electrical efficiency
$\eta_{e,ORC}$	ORC unit electrical efficiency
$\eta_{glob,CCHP}$	CCHP global efficiency
η_m	mechanical efficiency
η_{opt}	optical efficiency
$\eta_{opt,max}$	maximum optical efficiency
$\eta_{ORC,el}$	ORC unit electrical efficiency
$\eta_{ORC,th}$	ORC unit thermal efficiency
η_{REC}	receiver efficiency
η_{SF}	overall conversion efficiency of the solar field
η_{TES}	TES efficiency
σ	solar azimuthal angle
θ	solar incident angle

who have considered solar power as the potential dominant source of electricity in a 2010–2100 scenario limiting global warming to 2 °C. Especially solar thermal systems and photovoltaic panels have reached a mature state of development and present a positive economic feasibility. However, even Concentrated Solar Power (CSP) is increasing its attractiveness also for residential applications and it has been already considered by many researchers, particularly for remote and off grid installations. CSP consists in the concentration of solar radiation into a smaller area in order to achieve higher temperature levels compatible with more sophisticated applications than the mere domestic use of heat, as e.g. industrial processes, power generation, cooling. In the last years, the potential of CSP technologies, even at small scale, has been recognized both for Combined Heat and Power (CHP) and combined cooling heat and power (CCHP) applications [2] and it is especially appreciated in areas inadequately served by conventional power stations, where off-grid poly-generation systems are more advantageous than extending a power line (whose cost ranges from $15,000 to $50,000 per mile) [3].

A rising interest towards design, test and optimization of these systems emerges from literature studies. Different system configurations have been proposed with respect both to the solar collectors and to the final use of solar energy. As regards the different ways of collecting the solar radiation, five CSP technologies are available at present: Parabolic Trough Collector (PTC), Solar Power Tower (SPT), Parabolic Dish System (PDS), Linear Fresnel Reflector (LFR) and Compound Parabolic Collector (CPC) [4]. The concentration ratio and the overall performance of such technologies significantly differ from each other also due to the solar radiation that each system is able to collect. Among them, Parabolic Trough Collector is one of the most performing CSP technology with many applications [5], while Linear Fresnel Reflector is becoming more and more important for both industrial heating and electricity generation [6]. LFR is a line-focus CSP technology, as PTC, but differently from the latter, it has a lower impact in terms of cost of technology, thanks to a lighter and simpler structure [7]. Compound Parabolic Collector, instead, is able to collect both direct and diffuse solar radiation without a tracking system, differently

from LFR, and it proved to be a suitable option due to its low cost and good thermal performance at low and medium temperature ranges [8]. As a consequence, both technologies i.e. LFR and CPC, are expected to have an interesting market potential in the contest of nearly zero energy buildings in the next future [9].

In combination with CSP technologies, Organic Rankine Cycle systems are usually adopted at small scale to efficiently convert the solar energy into power [10]. Several studies in literature have been focused on the application of ORC systems driven by CSP. For example, Desai et Bandyopadhyay [11] have focused their attention on the proper selection of working fluids for solar ORC. Similarly Quolin et al. [12] designed the main components of a low-cost solar ORC with particular focus on the scroll expander and compared its performance with those of two different expansion machines by varying the working fluids. Taccani et al. [13] designed and experimentally evaluated the performance of a small-scale ORC plant using a scroll expander and powered by a $100\,m^2$ PTC solar field, they found a gross electricity efficiency of 8%. Bouvier et al. [14], instead, studied and tested the performance of a single-cylinder expander coupled with a $46.5\,m^2$ area double-axis PTC solar field obtaining an electrical power output of 1.3 kW and a solar-to-electricity efficiency of 3%. At large scale, instead, Ghasemi et al [15] investigated an hybrid solar-geothermal power generation plant aimed at increasing the overall efficiency of the ORC plant.

With reference to the built environment, Freeman et al. [16] focused their attention on a small scale CHP system for domestic use in UK and compared the performance of the plant coupled with PTC or evacuated tube collectors of the same array area. Ramos et al. [17] carried out a complete system optimisation of a non-regenerative sub-critical ORC unit with two different solar collector arrays to be used in a domestic environment. According to their simulation, a $60\,m^2$ evacuated-tube solar field coupled with the proposed ORC engine is able to obtain an electrical and thermal production of 3'605 kWh/year and 13'175 kWh/year respectively for the city of Athens with a levelised cost of energy close to that of PV systems. In another paper, Freeman et al. [18], stressed the key role of the Thermal Energy Storage (TES) in buffering the intermittent input of the solar energy in a domestic non-concentrated solar-ORC combined heat and power system in UK. A TES, indeed, is of paramount importance to increase the annual energy production of a solar ORC and ensure its normal operation. Therefore, over the years many researchers have focused their attention on this topic and on latent heat TES in particular. For example, Manfrida et al. [19] developed a mathematical model of a TES with Phase Change Material (PCM) and evaluated its use in a PTC-ORC, finding an overall solar-to-electricity efficiency of 3.9% over a week-period. Esen et al., instead, first developed a numerical model of a cylindrical TES for different PCMs [20] and then carried out an optimization study to design the geometry of a cylindrical latent heat TES for domestic heating purposes [21]. Furthermore, the same author [22], theoretically and experimentally, investigated its application in a solar assisted heat pump system for heating production.

While there are several works in literature regarding small scale CSP systems coupled with ORC units for cogeneration applications, to the best of the authors' knowledge only few articles referred to such systems for trigeneration purposes and none of them by means of absorption chillers. For example, Boyaghchi et Heidarnejad [23] performed a thermoeconomic analysis and a multi-objective optimization of a novel solar powered trigeneration system based on a 2.7 kWe ORC unit for electricity production and an ejector refrigeration cycle for cooling during summer. Karellas and Braimakis developed a thermodynamic model and an economic analysis of a trigeneration system based on the operation of an ORC and a vapor compression cycle powered by a biomass boiler and a solar PTC [24]. Compared to CCHP plants using electric chillers, thermally driven absorption chillers require a lower amount of electric energy and can exploit the huge amount of medium temperature thermal energy collected by the solar field during summer season. For this reason, in the recent years, some of

the authors of the present work have studied the main technical aspects and economic benefits of a CCHP solar system [25], consisting of a $50\,m^2$ CPC solar field, a 3.5 kWe ORC unit and a 17.6 kWc absorption chiller. They found that a proper setting of the system, in terms of temperature operating ranges, can be very effective to increase the overall energy produced by the CCHP system. However, they also highlighted that an adequate size of the solar field area is of paramount importance to achieve a significant energy production and exploit the ORC system at its best.

Due to the variability of energy production with ambient and operating conditions, in this paper the energy performance of the trigeneration plant previously analyzed by the authors has been first evaluated in two different locations in Italy, representative of the European Mediterranean area, and then compared to a similar trigeneration system based on the prototype conceived in the Innova MicroSolar Horizon 2020 research project [26], where LFR is used for the solar field. The final purpose of this analysis, indeed, is to provide useful insights into the adoption of small scale concentrated solar ORC trigenerative systems at residential level and highlight the importance of proper technology selection with different radiation conditions. Hence, the main novelties of the present paper rely on: (i) the investigation of two small-scale solar systems, that are going to be experimentally tested in the near future, in CCHP set-up; (ii) the evaluation of the influence of the incident radiation on the performance of the two trigeneration systems based on different solar technologies. Indeed, the Direct Normal Irradiance (DNI), as a component of the Global Horizontal Irradiance (GHI), has been demonstrated to be a decisive factor for the design of solar systems [27]. Furthermore, distribution and magnitude of DNI is very dependent on the atmospheric conditions, i.e. cloud amounts and precipitation level, as shown by Mohammadi and Goudarzi [28]. This fact has an impact on the performance and the continuous operation of CSP systems. Therefore, in the present work, the performance of the two mentioned CCHP systems has been comparatively evaluated in two distinct locations with the same Global Horizontal Irradiance but different ratios between Direct Normal Irradiance to Diffuse Horizontal Irradiance (DHI).

Hence, the paper is organized as follows: after the introduction, the methodology is presented in Section 2 and then a description of the two plants considered in this analysis is provided in Section 3. In Section 4 the models of the plants are described, while Section 5 reports the results of the analysis. Eventually, the last section summarizes the main conclusions.

2. Methodology

In this paper two distinct small-scale CCHP plants are investigated: Plant 1 is based on CPC-ORC technology coupled with a sensible heat TES, whilst Plant 2 consists of a LFR-ORC system and a latent heat TES. Both plants have the same collecting area of about $146\,m^2$ and the same size of the absorption chiller, equal to 17.6 kWc, in order to make a fair comparison of their performance in trigenerative configuration.

The performance of the systems is evaluated in two different locations in the Southern Italy, which can be considered representative of the European Mediterranean area: Napoli and Messina. Both locations have the same global irradiance (almost $1700\,kWh/m^2$), but they show a significant difference in the ratio between the direct normal irradiance to the diffuse horizontal irradiance. With more detail: (i) Napoli (local coordinates 40° 85′ 17.75″ N and 14° 26′ 81.24″ E) has a global irradiance of about $1682\,kWh/m^2$ and a ratio of DNI to diffuse irradiance, R_{irr}, of 1.478, and (ii) Messina (local coordinates 38° 19′ 38.14″ N and 15° 55′ 40.15″ E), despite a similar global irradiance, namely $1695\,kWh/m^2$, has a value of R_{irr} of about 2.481. Dynamic simulation models have been set up in order to analyse the behaviour of the considered systems by varying the ambient conditions. Main subroutines of the models were checked with first available lab test, while they will be extensively validated in the next future by means of

experiments on the field. Weather data have been taken from Meteonorm database on an hourly basis, while the simulation time step fixed to 10 min.

Firstly the performance of both plants is presented separately, focussing on typical working days in winter and summer seasons, so to highlight the influence of the solar radiation and the configuration of the plant. Secondly, the annual and monthly performance of the plants has been compared with reference to conversion efficiencies, energy production and operating hours. Eventually, because of the key role played by TES in solar ORC plants, the analysis of the influence of the considered TES technologies on the performance of the corresponding plants has been carried out.

3. Description of the plants

3.1. Plant 1

Apart from the size of the solar field, the plant has the same specifications as the real experimental system designed and tested by some of the authors. In particular, it consists of: (i) a 146 m^2 Compound Parabolic Collector solar field produced by Kloben Sud [29]; (ii) a diathermic oil storage tank of 3 m^3; (iii) a 3.5 kW regenerative Organic Rankine Cycle unit manufactured by Newcomen; and (iv) a 17 kWc Yazaki Energy System [30] absorption chiller (Fig. 1). As regards the solar field, the absorbing surface of the collectors is made of Al–N/Al selective material having an absorptance coefficient β > 0.92 and an emittance coefficient ε < 0.065. Copper tubes for high vacuum applications allow to achieve heat fluid temperatures up to 200 °C. A diathermic oil storage tank using therminol 62 as thermal vector [31] is used to decouple solar field and ORC unit.

The ORC unit operates according to a regenerative cycle using R245fa as working fluid. The related expander is a three radial cylinders alternative engine. The thermal power output from the ORC unit is recovered for heating and cooling purposes depending on seasonality. In the hot season, the rejected heat is directed to the absorption chiller to provide cold water to the user at nominal temperatures of about 7 °C. In terms of performance, the absorption chiller has a nearly 0.7 nominal coefficient of performance (COP) with an inlet hot water of 88 °C. However, it is able to work with acceptable performance up to a minimum inlet water temperature of about 70 °C, representing a good compromise for the operation of the overall system.

3.2. Plant 2

Plant 2, instead, is based on the innovative micro-CHP plant, developed by the consortium of several Universities and industrial organizations under the EU funded Innova Microsolar project [26]. In this work a trigeneration configuration is assumed. Therefore, it consists of: (i) a 146 m^2 concentrated LFR solar field, with 240 m^2 gross encumbrance, producing heat at temperatures in the range 250–280 °C; (ii) a 3.2 kWe Organic Rankine Cycle plant; (iii) an advanced PCM thermal storage tank equipped with reversible heat pipes; and (iv) a 17.6 kWc absorption chiller (Fig. 2).

The receiver consists of evacuated tube collectors placed at about 3.5 m from the ground and able to reach a maximum operating temperature of 400 °C. At nominal operating conditions (DNI equal to 900 W/m^2) the peak thermal power output is about 80 kWt as declared by the manufacturing company [32]. The ORC unit designed by EN-OGIA [33] operates accordingly to a regenerative cycle using NOVEC 649 as working fluid [34]. The TES system, as designed by Northumbria University and Aavid Thermacore [35] and investigated by Lleida University [36], consists of 3.8 tons of nitrate solar salt kNO$_3$ (40 wt %)/NaNO$_3$ (60 wt%), whose melting temperature is in the range 216–223 °C [37]. It has a heat storage capacity of about 100 kWh latent heat in order to guarantee 4 h of ORC unit operation during night time with a nominal input power of 25 kW. Reversible heat pipes, as developed by Aavid Thermacore [35], are adopted to transfer heat both from the solar field to the storage tank and from the storage tank to the ORC unit, depending on the operating conditions. Based on the solar radiation and the state of charge of the TES, the plant is able to switch from an operation mode to another according to the control system developed by S.TRA.TE.G.I.E. srl [38].

In addition, the 17.6 kWc Yazaki absorption chiller, as in the case of Plant 1, was considered to produce chilled water by recovering the thermal output power of the ORC unit in summer.

4. Description of the models

The models of the two plants described above have been developed in TRNSYS [39]. Despite TRNSYS has many library built-in components, ad-hoc subroutines have been developed by the authors in Matlab [40] for modelling the main components. In this work, both plants operate to produce electricity, while the thermal load is considered a
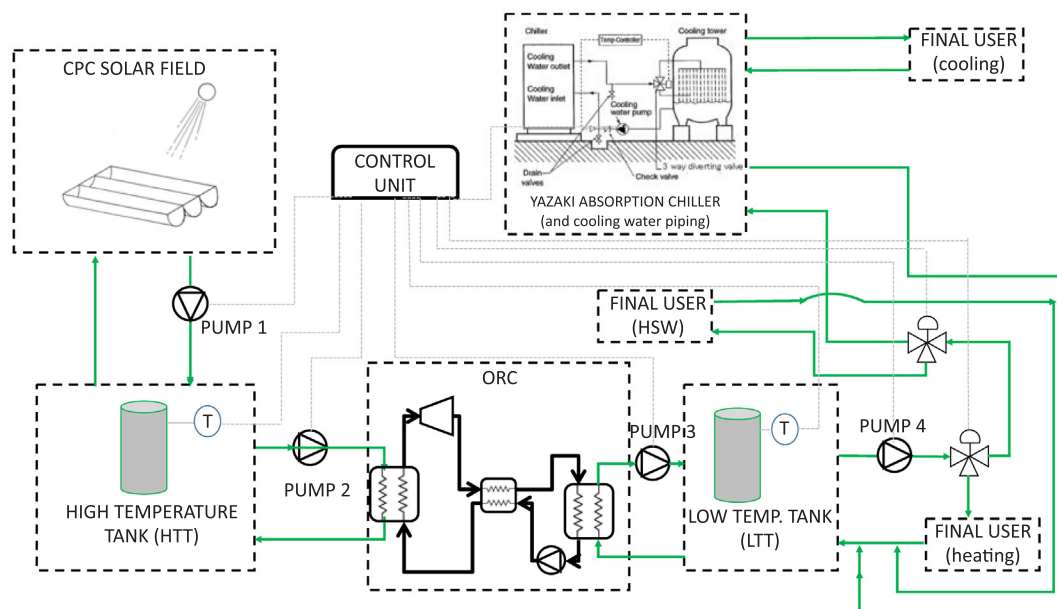

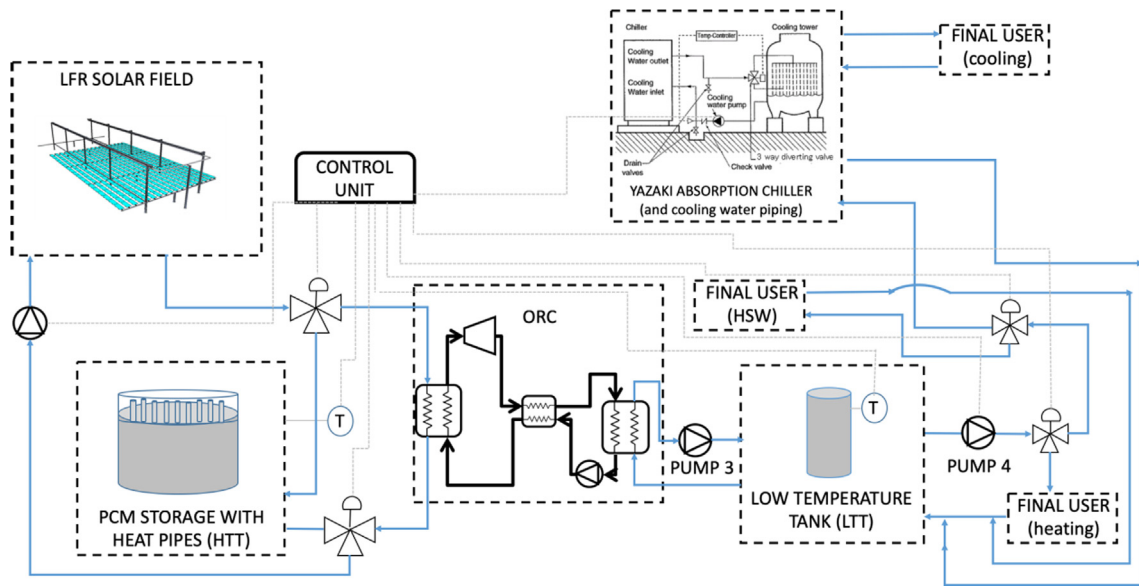**Fig. 1.** Functional scheme of Plant 1.

Fig. 2. Functional scheme of the Plant 2.

by-product which can be entirely collected and used for space heating, hot water or cooling depending on seasonality. According to the Italian decree 412/93 [32], which fixes the heating period for the different locations in Italy, the heating period corresponds to 15 November – 31 March in Napoli and 1 December – 31 March in Messina. The cooling period, instead, was assumed to be the same for both locations and it goes from 1 June to 30 September. As regards the set-points temperatures at the ORC condenser, they have been fixed to satisfy the heating and cooling needs of the building, assuming a radiant floor distribution systems. The thermal energy produced by the ORC is stored in the low temperature tank (LTT). The LTT set-point temperature ranges from 28 to 33 °C in winter. In the mid-season, when there is neither heating nor cooling demand, the energy from the ORC is used to satisfy the domestic hot water demand and the LTT temperature varies between 50 and 55 °C. In summer the LTT temperature range is 70–75 °C to supply adequate thermal power to the absorption chiller. The operation of the mixers and the diverters, as reported in Figs. 1 and 2, depends on seasonality.

Further details are provided in the following sections.

4.1. Plant 1

As regards the model of Plant 1, it consists of the following main components: Type 71 for the CPC solar field; Type 4 for both the diathermic oil tank (HTT) and the hot water storage tank (LTT), Type 155 for calling the ORC subroutine developed in Matlab, Type 107 for the absorption chiller and Type 510 for the evaporative cooling tower.

According to the CPC model in TRNSYS, the useful thermal power from the solar field $P_{SF,out}$ is equal to:

$$P_{SF,out} = A \cdot (\eta_0 \cdot (G_b \cdot K_\theta + G_d \cdot K_d) - a_0 \cdot (T_m - T_a) - a_1 \cdot (T_m - T_a)^2) \quad (1)$$

where A is the collector area, G_b and G_d the direct and diffuse radiation on collector plane, K_θ and K_d the Incident Angle Modifier (IAM) for direct and diffuse radiation respectively, T_m the mean temperature of the fluid in the collector, T_a the ambient air temperature and η_0 the maximum optical efficiency. Finally, a_0 and a_1 are coefficients which depend on type and model of the collectors considered and they are equal to 0.974 and 0.005 W/m^2·K respectively in this case.

With reference to the ORC unit, it has been modelled considering steady state conditions based on the following assumptions: (i) a minimum driving temperature difference between the evaporator and the condenser equal to 50 °C; (ii) a minimum temperature difference of

34 °C between the inlet diathermic oil and the evaporating temperature; (iii) an overheating of 5 °C and a maximum evaporation temperature of 149 °C (iv) a minimum pressure ratio at the expander of 2.5 and a maximum inlet pressure of 25 bar; and (v) an expander isentropic efficiency varying in the range 46–60% and an isentropic efficiency of the pump equal to 70%. Moreover, pressure drops and thermal capacity of the components have been neglected, whilst efficiency of the heat exchangers fixed constant. In particular, the evaporator has been modelled according to the ε-NTU method, while the exact characterization of the heat transfer coefficients in the different regions of the vapour generator neglected.

Hence, the electric power produced by the ORC is equal to:

$$P_{ORC,el} = \dot{m}_f \cdot [\eta_m \cdot \eta_{el} \cdot \Delta h_e - \Delta h_p / (\eta_m \cdot \eta_{el})] \quad (2)$$

where $\dot{m}_f$ is the organic fluid flow rate, η_m and η_{el} the mechanical and electric efficiencies assumed equal to 95% and 90% respectively, Δh_e and Δh_p the actual specific enthalpy difference across the expander and the pump.

With regard to the output thermal power, it is evaluated as in Eq. (3):

$$P_{ORC,out} = \dot{m}_c \cdot c_{p,c} \cdot (T_{out} - T_{in}) \quad (3)$$

with $\dot{m}_c$ the water flow rate, $c_{p,c}$ the specific heat of the water and T_{out} and T_{in} the outlet and inlet temperatures of the water at the condenser.

In particular, a minimum temperature difference between the inlet temperature of the cooling water and the condensing temperature of the working fluid has been fixed equal to 12 °C.

The cooling power of the absorption chiller is equal to Eq. (4):

$$P_{abs} = P_{abs,in} \cdot COP \quad (4)$$

where $P_{abs,in}$ is the inlet thermal power and COP depends on the operating conditions.

Table 1 reports the operating conditions of Plant 1 where HTT_ΔT are the working temperature ranges of the HTT storage. As shown in a previous work by the authors [25], the proper choice of this adjustment parameter has remarkable effect on system performance. When the temperature available at the HTT storage tank reaches the highest bound, the ORC unit switches on, while when it goes below the lowest bound, the ORC unit switches off. Three optimal values of this temperature range have been fixed respectively for hot, cold and mid seasons. The mass flows reported in Table 1 regard the pumps visible in Fig. 1.

Table 1
Operating conditions of Plant 1.

Operating conditions	Value
HTT_$\Delta T_{hot\ season}$	170–160 °C
HTT_$\Delta T_{cold\ season}$	120–110 °C
HTT_$\Delta T_{mid\ season}$	160–135 °C
Mass flow rate of PUMP1	7000 kg/h
Mass flow rate of PUMP2	1800 kg/h
Mass flow rate of PUMP3	3600 kg/h
Mass flow rate of PUMP4	4320 kg/h
Cooling water pump	9180 kg/h

4.2. Plant 2

With respect to Plant 2, the following main components have been included into the model: (i) the LFR solar field; (ii) the micro ORC plant; (iii) the PCM thermal energy storage tank equipped with reversible heat pipes; (iv) the absorption chiller. In this case, specific subroutines for the LFR solar field and the PCM storage tank equipped with heat pipes have been developed by the authors in Matlab in addition to that of the ORC unit. As for the model of Plant 1, Type 107 and Type 510 have been used to model the absorption chiller and the evaporative cooling tower. Finally, mixers and diverters are included into the model to divert the flow of the oil according to the operation mode of the plant.

The performance of the LFR solar field has been assessed in terms of its optical efficiency under quasi-steady state conditions. The maximum optical efficiency of the LFR is reached when the incident angle is zero and can be expressed as in Eq. (5):

$$\eta_{opt} = \eta_{opt,max}(\theta = 0) \cdot IAM(\alpha, \sigma) \tag{5}$$

where θ is the solar incident angle, α the solar elevation and σ and the azimuthal angle. The values of IAM for the considered collector have been provided by the manufacturing company ELIANTO [32] at different solar elevation and azimuthal angles.

Therefore, taking into account the thermal losses of the absorber tubes, Q_{loss}, the collected thermal energy of the LFR can be calculated as in Eq. (6):

$$P_{SF,out} = A \cdot DNI \cdot cos(\theta) \cdot \eta_{opt} \cdot \eta_{rec} - Q_{loss} \tag{6}$$

where A is the area of the primary collectors, cos(θ) the cosine of the solar incident angle and η_{rec} the receiver efficiency.

The oil flow rate in the solar field is adjusted in order to keep the oil temperature at 210 °C when the solar field supplies the ORC, thus assuring a good electric conversion efficiency of the ORC unit or at 10 °C more than the average PCM TES temperature in case the solar field supplies the storage.

The model of the ORC unit is similar to that of Plant 1 considering: (i) a constant temperature difference between the inlet oil from the plant (LFR and or TES) and the evaporating temperature of the working fluid equal to 34 °C if the cycle is subcritical (otherwise the evaporating temperature is set 5 °C lower than the critical temperature); (ii) a minimum superheating of 5 °C at the evaporator outlet; (iii) no subcooling at the condenser; and (iv) pump and turbine isentropic

efficiencies varying with operating conditions according to the data provided by the manufacturing company ENOGIA [33].

The PCM storage tank has been modelled according to the guidelines of the IEA Task 32 report on advanced storage concepts [41], where a detailed description of Type 185 is provided. The model is based on the following main assumptions: (i) material isotropic and isothermal in each internal time-step; (ii) no hysteresis and subcooling effects; and (iii) charging and discharging not simultaneous. The presence of heat pipes is modelled by both limiting the maximum power exchanged to 40 kW and fixing a minimum temperature difference between the oil and the PCM equal to 5 °C.

Hence, the temperature variation of the PCM due to the heat exchanged is given by:

$$\Delta T_{PCM(t+1)} = \Delta T_{PCM(t)} \cdot e^{-[\Delta t_{int-timestep} \cdot k]} \tag{7}$$

where k is a function of both PCM and oil thermal properties [41]. Then, from the temperature variation of the PCM, it is possible to calculate the heat exchanged as:

$$Q_{PCM(t+1)} = \int_{t}^{t+1} Q_{PCM(t)} \cdot dt \tag{8}$$

The model of the absorption chiller is the same as in Plant 1.

The operation mode of the plant depends on the solar radiation and the state of charge of the TES. The diathermic oil from the solar field flows to the PCM TES and/or directly to the ORC depending on its temperature and on the amount of power collected at the receiver. On the contrary, when the power produced by the solar field is low or zero and the average PCM TES temperature is within a given operating range ($T_{ORC,on} = 217$ °C and $T_{ORC,off} = 215$ °C), the thermal energy of the TES can be used to run the ORC unit and assure its operation for a maximum of 4 h with no sun. Table 2 reports set-points and threshold values of each operation mode (OM).

Further details on the plant model can be found in [42].

5. Results and discussion

In order to evaluate the influence of the incident solar radiation on the performance of the integrated systems, both plants have been investigated for the above mentioned two different Italian locations. The performance of the plants has been evaluated in terms of electric and thermal energy production on a monthly and yearly basis. Furthermore the following conversion efficiencies have been assessed: (i) the solar field efficiency (η_{SF}), defined as the ratio between the output power from the solar collector and the input solar power; (ii) the electric efficiency of the ORC ($\eta_{ORC,el}$), defined as the ratio between the output electric power and the inlet thermal power to the ORC; (iii) the thermal efficiency of the ORC ($\eta_{ORC,th}$), defined as the ratio between the output and input thermal power of the ORC; (iv) the thermal energy storage efficiency (η_{TES}), defined as the ratio between the outlet thermal energy towards the ORC (discharging) and the inlet thermal energy from the solar field during its charging; and finally (v) the coefficient of performance (COP), i.e. the ratio between the cooling power and the input thermal power of the absorption chiller.

Table 2
Operating conditions for the different operation modes of Plant 2.

Operation Mode	Description	Operating conditions
OM1	LFR supplies ORC	$T_{oil} = 210$ °C
OM2	System off	–
OM3	LFR supplies PCM TES	$T_{oil} = T_{TES,av} + 10$ °C
OM4	LFR supplies PCM TES and ORC	$T_{oil} = 210$ °C if $T_{TES,av} < 200$ °C or $T_{TES,av} > 280$ °C otherwise $T_{oil} = T_{TES,av} + 10$ °C if $T_{TES,av} > 200$ °C
OM5	PCM TES supplies ORC	oil flow rate 0.22 kg/s
OM6	PCM TES and LFR supply ORC	$T_{oil} = 210$ °C and oil flow rate 0.22 kg/s

In the following sections the results for each plant, first, and then their comparison, are reported.

5.1. Plant 1

Fig. 3a and b report the energy breakdown of Plant 1. The overall monthly energy values are very similar for the two considered locations. As expected the output energy from the solar field is much lower than the input solar radiation, while it is equal to the input energy to the TES, because of the plant configuration. Furthermore the higher solar contribution in summer rather than in winter is evident. In summer period (June-September), it is visible the energy produced by the absorption system, which causes a corresponding decrease of the electric energy output compared with the mid-season period. Indeed the highest electric energy production is achieved in the mid-season, when there is a higher temperature difference between the ORC hot source (HTT) and cold sink (LTT). On the contrary, the highest thermal energy output from the ORC unit is obtained in the hot season, thus positively contributing to the cooling production.

From the analysis of the results reported in Tables 3 and 4, it is evident that the performance of Plant 1 is not significantly affected by the considered location. More precisely, the conversion efficiency of the solar field is weakly influenced by location in case of CPC technology. Indeed, the mean annual conversion efficiency of the solar field is the same (36.2%) for the two cities. Even the conversion efficiency and the operating hours of the ORC unit (and, as a consequence the thermal and electric energy output) are more or less the same in the two considered locations, proving that such system is not affected by the ratio between the DNI to the diffuse irradiance. For example, the electric efficiency ranges between 3.0 and 7.4% in Napoli and between 3.0 and 7.1% in Messina.

The performance of the plant has been then analysed on an hourly basis for typical working days in winter and summer as reported in Fig. 4a-d. The collected thermal energy from the solar field during a typical winter day is enough to supply the ORC unit almost at its nominal operating conditions (Fig. 4a and c). Moreover, with reference to Fig. 4a, it is evident that even low thermal input and output power from the solar field are beneficial for the operation of the plant. Indeed, in the period 1 pm–2 pm, when the solar radiation is low, the TES discharges energy to the ORC unit, whilst at a certain time after 2 pm the ORC is switched off and the TES charged. Hence, the TES helps to balance the system by reducing the effect of solar irradiance variation. Despite a higher solar irradiance than in wintertime, in summer season the ORC unit is prone to frequent on-off in Napoli. This is due to difficulty of the absorption chiller to use all the thermal energy available at the condenser, then the condensing temperature rises and the system shuts down for security reasons. Looking at the solar input power at the

collector in Messina and Napoli, it is evident that they are very similar and this aspect justifies the finding that such a solar collector is less influenced by the plant location. Indeed the electrical and thermal output power of the ORC in Messina and Napoli, as said, are similar. Finally, thanks to the LTT, the absorption chiller has a lower tendency to interruptions compared to the ORC unit in both locations.

5.2. Plant 2

Fig. 5a-b report the monthly energy balance for Plant 2. Because of the plant configuration and operating strategy, the output thermal energy from the solar field goes mostly to the ORC unit and only a reduced amount is directed to the PCM TES. The electric and thermal energy production of the ORC unit varies substantially during the year: while it is very poor in winter, from April to September it grows significantly and especially the electricity production maintains a stable production value.

As reported in Tables 5 and 6, indeed, the conversion efficiencies and the operating hours of the system change with location, thus proving that such system is affected by the ratio of the DNI to the DHI. Indeed, its performance are considerably higher in Messina rather than in the city of Napoli. In particular, due to the higher ratio between DNI to diffuse irradiance, R_{irr}, in Messina: (i) the mean annual conversion efficiency of the solar field is about 2.7% higher than in Napoli; (ii) the ORC unit works around 500 operating hours more; (iii) the electrical and thermal energy production of the ORC unit are about 19% higher; and (iv) the operating hours of the absorption chiller are almost 15% higher.

As regards the TES, because of the plant operation mode, the mean annual efficiency (η_{TES}) is significantly lower compared to that of Plant 1. In winter, indeed, the TES temperature remains often below the melting point and, as a consequence, the stored energy is not usefully exploited.

In general, the performance of the ORC unit in Plant 2 strictly depends on the operation modes (discussed in Section 4.2) which in turn are related to the solar radiation and state of charge of the TES. More precisely: in OM1 the LFR supplies the ORC only, in OM4 the LFR supplies both the TES and the ORC, in OM5 the TES supplies the ORC, while in OM6 both the TES and the LFR supply the ORC. In Table 7 the performance of the ORC unit are reported with respect to the operation modes for the city of Messina.

In Table 7, the performance of the Plant in OM1 has been omitted, since this operation mode is limited to about 88 h/year and it occurs in between the other operating modes (e.g. before OM4, when the solar power is so high to supply not only the ORC, but even the TES). Consequently, the thermal energy input to the TES is very low and the electric energy and efficiency close to zero. From the analysis of the
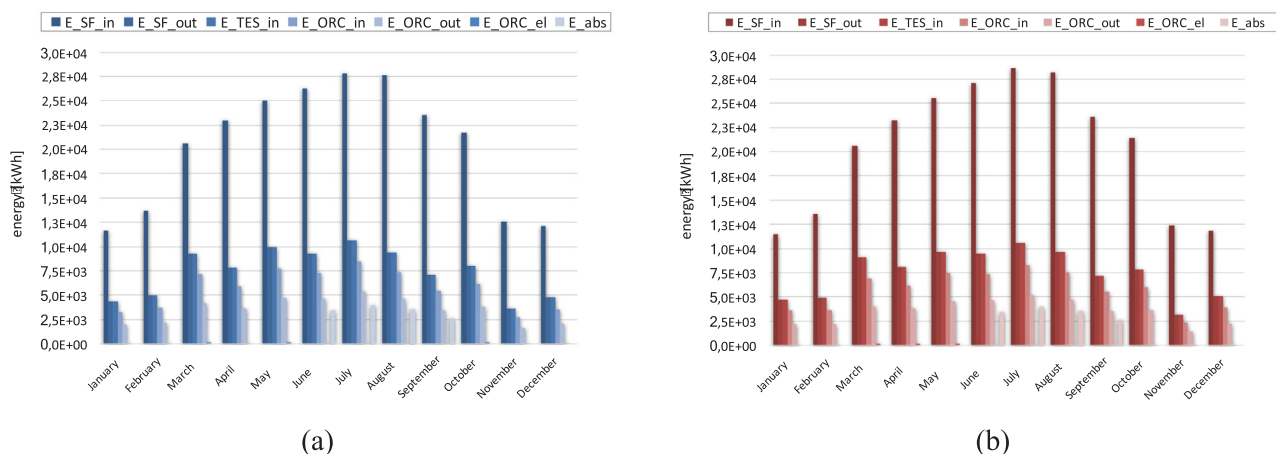

Fig. 3. Monthly energy balance of Plant 1: (a) in Napoli; (b) in Messina.

Table 3
Monthly performance of Plant 1 for the city of Napoli.

Month	η_{SF} [%]	$\eta_{ORC,el}$ [%]	$\eta_{ORC,th}$ [%]	η_{TES} [%]	h_{ORC}	$E_{ORC,el}$ [kWh]	$E_{ORC,out}$ [kWh]	COP	h_{abs}	E_{abs} [kWh]
Jan	36.8%	6.1%	73.5%	100.0%[a]	92.0	196.1	2381.7	–	–	–
Feb	36.3%	5.9%	73.5%	98.2%	104.3	217.3	2687.0	–	–	–
Mar	45.1%	7.4%	71.1%	99.3%	181.8	534.4	5108.7	–	–	–
Apr	33.8%	5.4%	75.1%	97.8%	157.7	318.8	4421.2	–	–	–
May	39.8%	5.8%	74.5%	99.2%	191.3	447.8	5782.3	–	–	–
Jun	35.4%	3.0%	77.9%	97.9%	182.2	215.4	5647.3	0.65	214.0	3407.3
Jul	38.0%	3.0%	78.1%	99.2%	206.0	246.4	6566.0	0.64	252.6	4011.2
Aug	33.9%	3.0%	77.6%	99.1%	195.5	223.1	5717.3	0.64	220.2	3497.1
Sep	30.0%	3.1%	77.8%	98.0%	147.8	167.0	4259.6	0.65	163.7	2605.0
Oct	36.8%	5.6%	75.0%	99.6%	161.4	345.1	4641.1	–	–	–
Nov	28.6%	5.6%	74.6%	98.3%	75.3	150.2	2004.2	–	–	–
Dec	39.9%	6.4%	72.9%	97.8%	98.3	226.8	2595.9	–	–	–
Total	**36.2%**	**5.0%**	**75.1%**	**98.7%**	**1794.0**	**3288.5**	**51812.6**	**0.65**	**851.8**	**13520.6**

[a] Because of initialization.

Table 4
Monthly performance of Plant 1 for the city of Messina.

Month	η_{SF} [%]	$\eta_{ORC,el}$ [%]	$\eta_{ORC,th}$ [%]	η_{TES} [%]	h_{ORC} [h]	$E_{ORC,el}$ [kWh]	$E_{ORC,out}$ [kWh]	COP	h_{abs} [h]	E_{abs} [kWh]
Jan	40.9%	6.4%	72.5%	100.0%[a]	98.2	229.5	2600.0	–	–	–
Feb	36.0%	6.0%	72.6%	98.2%	102.5	218.8	2636.6	–	–	–
Mar	44.1%	7.1%	71.8%	98.4%	179.5	491.7	4945.1	–	–	–
Apr	34.6%	5.6%	75.1%	98.8%	162.2	345.2	4647.0	–	–	–
May	37.7%	5.6%	74.7%	99.2%	192.7	419.2	5596.2	–	–	–
Jun	34.7%	3.0%	77.8%	98.3%	188.7	218.3	5716.3	0.65	216.7	3451.3
Jul	36.7%	3.0%	77.8%	99.0%	211.3	243.9	6426.7	0.64	247.9	3936.3
Aug	34.0%	3.1%	77.6%	99.1%	198.7	229.8	5841.8	0.64	224.5	3564.4
Sep	30.2%	3.0%	77.8%	98.7%	147.8	169.5	4328.4	0.65	164.1	2609.7
Oct	36.3%	5.5%	74.9%	98.9%	158.8	327.5	4498.3	–	–	–
Nov	25.5%	5.5%	75.1%	94.9%	61.7	127.2	1743.5	–	–	–
Dec	43.1%	6.4%	72.1%	99.3%	105.0	248.9	2784.3	–	–	–
Total	**36.2%**	**5.0%**	**75.0%**	**98.6%**	**1807.0**	**3269.6**	**51764.1**	**0.65**	**853.2**	**13561.7**

[a] Because of initialization.

results reported in Table 3, it is evident that Plant 2 operates mostly in mode OM4 (2147 h), achieving a maximum monthly mean electric efficiency of the ORC of about 11.4% in March. Because of the different condensing temperatures during the year, the monthly mean electric output power in OM4 ranges from 1.78 kWe in September to 3.18 kWe in March, i.e. the electric efficiency is lower in cooling season when the LTT set-point depends on the absorption chiller operation. On the contrary, the thermal output power is almost constant throughout the year and achieves its maximum in July. Because of the set-point temperatures of the PCM TES, the ORC is able to achieve high conversion efficiencies also in mode OM6, when both the LFR and the TES supply thermal power to the ORC. However, this operation mode is limited to about 225 h/year and it does not occur in January and December, due to the limited surplus of solar radiation for charging also the TES. Even OM5, which reaches 801 h of operation annually, does not occur in December, whilst it is mainly present in summer season.

Fig. 6a-d, instead, report the daily performance trend. Despite a power input in the range 80–120 kWt during the morning of the considered winter day in Napoli (Fig. 6a), the daily performance is limited. This is due to the fact that the temperature of the PCM TES is too low to run the ORC unit (see Fig. 7a) and, as soon as the input solar power to the solar field goes down at noon, the ORC unit is switched off. On the contrary, for the city of Messina, thanks to the constant input thermal power throughout the considered winter day, the produced energy is higher and a small amount of energy is also supplied to the TES for its charging (Fig. 6c). Independently from the location, in summer, Plant 2 exhibits a very good performance especially because it generates electric and cooling power uninterruptedly, as evident in Fig. 6b and d. The prolonged radiation indeed allows to simultaneously run the ORC unit and charge the TES, thus extending the operation of the ORC and the

power production also after sunset. However, because of the higher condensing temperatures compared to winter season, the electric power output remains below 2 kWe. As regards the absorption chiller, its operation is prolonged also during night, thanks to the temperatures achieved in the LTT. The thermal output power of the ORC, indeed, is directed to the LTT and once its temperature is above the threshold value, the absorption chiller switches on.

5.3. Comparative analysis of the two plants

In this Section, the monthly performance of the two plants has been compared with the final aim to achieve a thoughtful understanding of their operation. In general, in the period October-April the output electric and thermal energy from the ORC unit is higher for Plant 1. On the contrary, in summer, independently from the location, the output energy is higher for Plant 2 and, as a consequence, also the cooling energy produced. Tables 4 and 5 report the mean monthly conversion efficiencies and energy output of Plant 1 for the city of Napoli and Messina, while Tables 6 and 7 those of Plant 2.

Although the higher irradiance and number of operating hours of the system during the hot season, for every plant the electric efficiencies of the ORC are lower in summer because of the higher condensation temperature necessary to run the absorption chiller. In particular, they are less than half of the electric efficiency achieved in winter time. This lower performance of the ORC unit is compensated by the cooling load obtained by means of the absorption chiller. Moreover, despite the lower electric efficiency of the ORC in summer, the electric energy production of Plant 2 is higher in summer rather than in winter in any case, whilst it is almost the same for Plant1 (with the exception of March) throughout the year. With reference to the results reported in
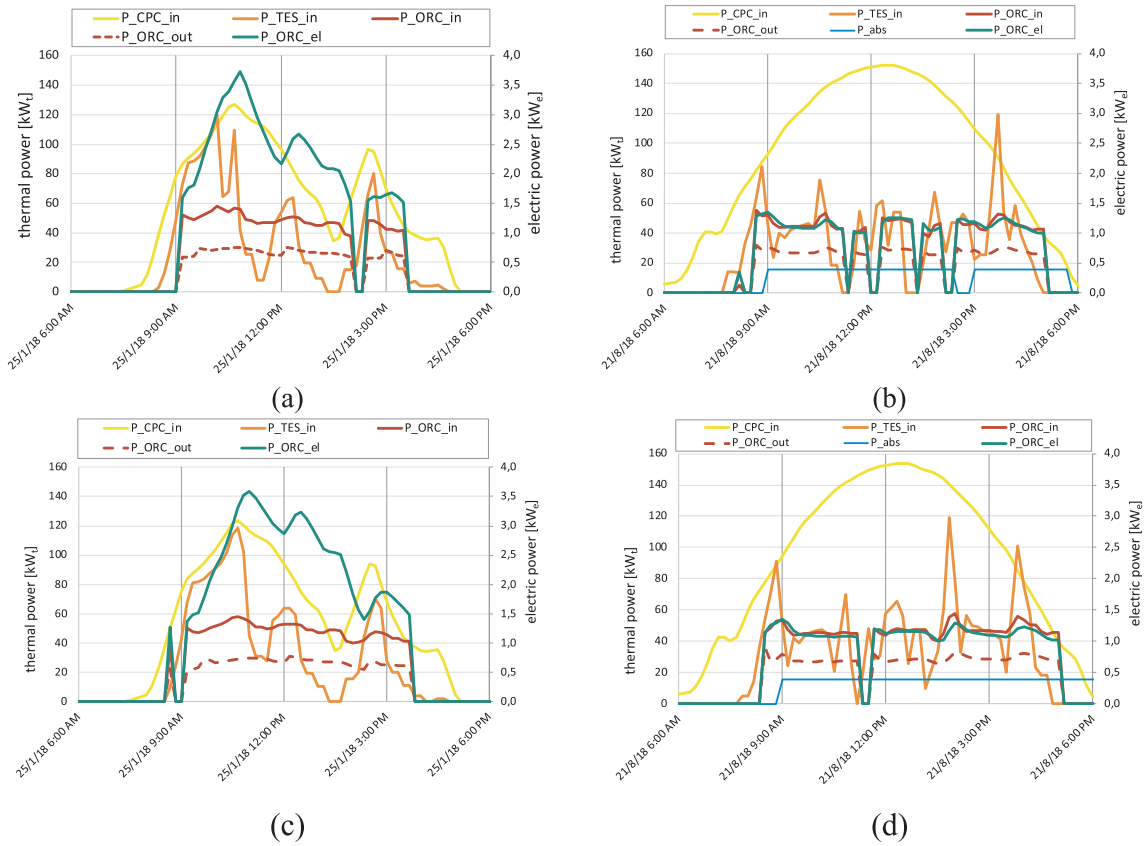
Fig. 4. Daily trend of performance of Plant 1 for typical days in (a) winter in Napoli, (b) summer in Napoli, (c) winter in Messina, (d) summer in Messina.
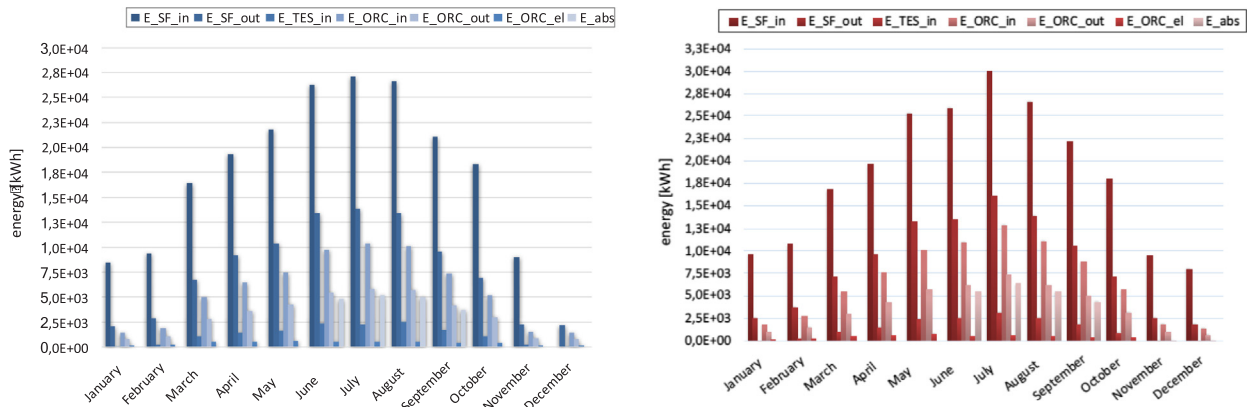

Fig. 5. Monthly energy balance of Plant 2: (a) in Napoli (b) in Messina.

Tables 3–6, it is evident that Plant 2 is much more affected by seasonality compared to Plant 1. Indeed, the conversion efficiency of the solar field of Plant 2 ranges from 22.9% in December to 51.1% in June for the city of Napoli and from 27.6% in January to 54.2% in July for Messina. On the contrary, the conversion efficiency of the CPC solar field of Plant 1 ranges from a minimum of 25.5% in November for the city of Messina to a maximum of 45.1% in March for Napoli. Therefore, the ratio between the maximum and the minimum mean monthly conversion efficiency is about 2.23 for the LFR solar field, whilst it is only 1.72 for the CPC.

Because of the higher operating temperatures of the PCM storage tank of Plant 2 compared to the HTT of Plant 1, the electric efficiency of the ORC ($\eta_{ORC,el}$) unit is significantly higher for the former and it achieves a mean value of 11.3% in December in Messina. In addition, Plant 2 is able to achieve a higher electrical production than Plant 1,

independently from the location. In particular, it is almost 75% higher in the case of Messina. Also the thermal energy production is higher than that of Plant 1 in Messina, whilst it is lower in Napoli. Because of the substantially higher conversion efficiency of the solar field in summer, the thermal energy production and the related cooling energy is higher for Plant 2 during this season. As a consequence, the cooling energy production of Plant 2 is significantly higher and around 60.8% more than that of Plant 1 for the city of Messina (about 21,808 kWh for Plant 2 and 13,562 kWh for Plant 1). Furthermore, with reference to Plant 1 the cooling energy production does not differ with locations. Therefore, in case of high DNI, LFR technology performs much better than CPC, resulting especially suitable for solar cooling applications.

Hence, the performance of both plants are in line with those reported in literature for similar systems. With reference to the city of Messina, Plant 1 achieves a peak solar-to-electricity electricity

Table 5
Monthly performance of Plant 2 for the city of Napoli.

Month	η_{SF} [%]	$\eta_{ORC,el}$ [%]	$\eta_{ORC,th}$ [%]	η_{TES} [%]	h_{ORC} [h]	$E_{ORC,el}$ [kWh]	$E_{ORC,out}$ [kWh]	COP	h_{abs} [h]	E_{abs} [kWh]
Jan	24.3%	11.1%	69.1%	100.0%[a]	55.2	162.2	1010.6	–	–	–
Feb	30.6%	11.1%	69.1%	60.8%	72.3	211.9	1317.0	–	–	–
Mar	40.7%	11.1%	69.1%	82.3%	192.5	550.4	3440.6	–	–	–
Apr	47.5%	8.5%	70.0%	79.2%	250.5	546.6	4485.8	–	–	–
May	47.5%	8.5%	70.0%	79.4%	290.2	634.0	5213.0	–	–	–
Jun	51.1%	5.2%	69.4%	83.0%	376.8	508.1	6740.6	0.71	278.5	4789.3
Jul	51.0%	5.3%	69.6%	81.9%	398.5	548.9	7191.8	0.71	300.8	5173.3
Aug	50.1%	5.2%	69.3%	85.2%	396.0	525.8	7005.1	0.71	287.8	4949.8
Sep	45.4%	5.3%	69.9%	83.4%	285.8	385.5	5121.9	0.71	213.0	3663.0
Oct	37.6%	8.5%	70.0%	78.2%	202.8	441.4	3633.2	–	–	–
Nov	24.5%	9.1%	69.5%	73.2%	58.7	139.0	1058.9	–	–	–
Dec	22.9%	11.0%	69.1%	87.0%	52.7	154.0	963.4	–	–	–
Total	**39.4%**	**8.3%**	**69.5%**	**81.3%**	**2632.0**	**4807.9**	**47182.1**	**0.71**	**1080.1**	**18575.4**

[a] Because of initialization.

Table 6
Monthly performance of Plant 2 for the city of Messina.

Month	η_{SF} [%]	$\eta_{ORC,el}$ [%]	$\eta_{ORC,th}$ [%]	η_{TES} [%]	h_{ORC} [h]	$E_{ORC,el}$ [kWh]	$E_{ORC,out}$ [kWh]	COP	h_{abs} [h]	E_{abs} [kWh]
Jan	27.6%	11.2%	69.2%	70.2%	68.8	207.9	1282.4	–	–	–
Feb	35.5%	11.1%	69.0%	68.3%	106.7	315.0	1950.5	–	–	–
Mar	42.2%	11.0%	69.1%	82.6%	205.8	588.5	3698.7	–	–	–
Apr	48.9%	8.5%	70.0%	81.3%	299.2	653.8	5363.4	–	–	–
May	52.0%	8.5%	69.9%	83.1%	399.2	858.2	7087.9	–	–	–
Jun	52.5%	5.2%	69.6%	83.5%	431.2	579.5	7691.7	0.71	319.0	5486.1
Jul	54.2%	5.1%	69.1%	86.4%	504.5	664.5	8929.7	0.71	369.6	6357.0
Aug	52.7%	5.2%	69.3%	87.1%	431.5	575.0	7685.0	0.71	321.5	5528.8
Sep	48.1%	5.3%	69.8%	82.1%	344.7	468.3	6181.3	0.71	258.0	4436.7
Oct	39.5%	8.5%	70.1%	78.3%	220.0	481.3	3985.8	–	–	–
Nov	27.9%	8.7%	70.5%	62.5%	72.8	164.9	1334.4	–	–	–
Dec	27.6%	11.3%	69.3%	6.5%	51.7	158.0	971.5	–	–	–
Total	**42.1%**	**8.3%**	**69.6%**	**72.7%**	**3136.0**	**5714.9**	**56162.2**	**0.71**	**1268.1**	**21808.7**

efficiency of about 7.5%, while Plant 2 of about 11%, which are comparable to the value stated by Taccani et al. [13] in the field tests of a 100 m² PTC-ORC plant and higher than the 3% experimentally reached by Bouvier et al. [14] in a 46.5 m² area double-axis PTC solar ORC. In the cogeneration configuration during the mid seasons, Plant 1 shows an average solar-to-electricity efficiency of about 2.0%, while Plant 2 of almost 4.0%, compared to the 3.9% reported by Manfrida et. [19] over a week-period (in July) for a PTC-ORC. On the contrary, in their study Boyaghchi et Heidarnejad [23] obtained for a solar CCHP system consisting of 2.7 kWe ORC and an ejector refrigeration cycle an overall (thermal) efficiency of 23.66% in summer and 48.45% in winter. In case of Plant 1 such efficiencies are about 18.15% and 29.82%, while for Plant 2 they are equal to 28.27% and 25.75% in summer and winter respectively.

In terms of energy production, it is difficult to compare the performance of the plants under investigation in this paper with those of the systems reported in literature, since the collecting area of the solar fields are usually different. However, as a rule of thumb, it can be stated that the electric energy production is similar to the values reported by Ramos et al. [17] and Calise et al. [43] in their simulations of solar ORC systems (respectively about 3600 kWh/year in the city of Athens and 4300 kWh/year in Napoli). Both these systems have a collecting area of the solar field lower than that of the plants here investigated but none of them are in trigenerative configuration, when the electricity production is expected to decrease.

Eventually, because of the key role played by TES systems in ensuring the proper operation of solar plants, a focus on their influence on the ORC unit of both plants have been carried out. The considered

Table 7
Performance data of ORC unit for Plant 2 with different operation modes in the city of Messina.

|		Jan	Feb	Mar	Apr	May	Jun	Jul	Aug	Sep	Oct	Nov	Dec	Working hours
OM4	$P_{ORC,in}$ [kW]	24.7	24.8	24.9	24.7	24.8	24.6	24.6	24.6	24.5	24.7	24.0	24.6	2147 h
	$P_{ORC,out}$ [kW]	18.5	18.9	19.2	19.7	19.9	20.5	20.7	20.6	20.4	19.6	18.6	18.3	
	$P_{ORC,el}$ [kW]	3.02	3.12	3.18	2.57	2.61	1.80	1.83	1.81	1.78	2.50	2.35	2.97	
	$Eff_{ORC,el}$ [%]	11.1	11.1	11.4	9.3	9.4	6.5	6.6	6.5	6.5	9.1	8.8	11.0	
OM5	$P_{ORC,in}$ [kW]	18.8	18.3	18.5	16.8	16.9	15.1	15.1	15.1	15.0	16.5	16.6	0.0	801 h
	$P_{ORC,out}$ [kW]	13.9	13.6	13.7	12.9	13.0	12.2	12.2	12.1	12.1	12.7	12.8	0.0	
	$P_{ORC,el}$ [kW]	1.85	1.75	1.77	1.08	1.11	0.38	0.39	0.37	0.36	0.98	1.04	0.0	
	$Eff_{ORC,el}$ [%]	9.5	9.2	9.2	6.2	6.3	2.4	2.4	2.4	2.3	5.7	6.0	0.0	
OM6	$P_{ORC,in}$ [kW]	0.00	22.77	21.90	20.63	21.90	18.97	19.09	20.08	19.39	21.06	21.04	0.0	225 h
	$P_{ORC,out}$ [kW]	0.00	16.81	16.19	15.72	16.70	14.99	15.13	15.87	15.30	16.06	15.99	0.0	
	$P_{ORC,el}$ [kW]	0.00	2.67	2.46	1.81	2.01	1.02	1.02	1.16	1.09	1.85	1.86	0.0	
	$Eff_{ORC,el}$ [%]	0.0	11.0	10.5	8.2	8.6	4.8	4.8	5.2	5.1	8.1	8.3	0.0	
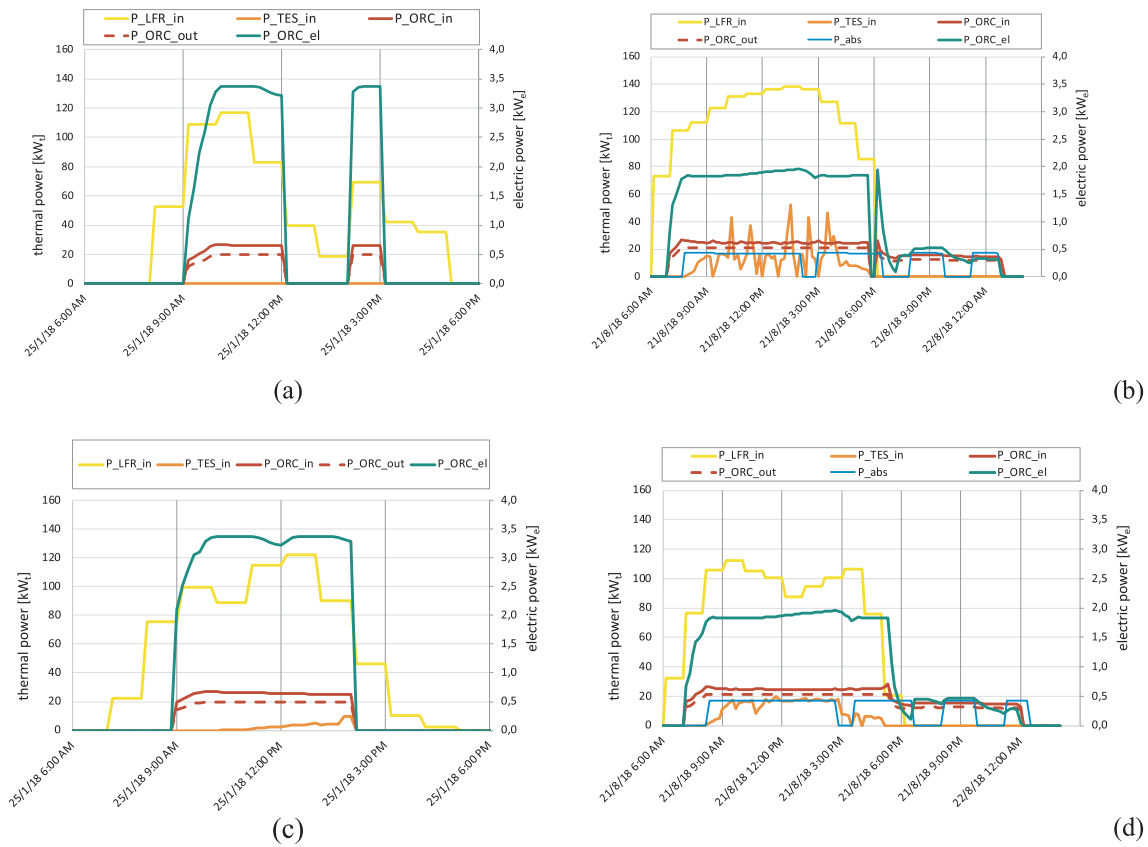
Fig. 6. Daily trend of performance of Plant 2 for typical days in (a) winter in Napoli, (b) summer in Napoli, (c) winter in Messina, (d) summer in Messina.
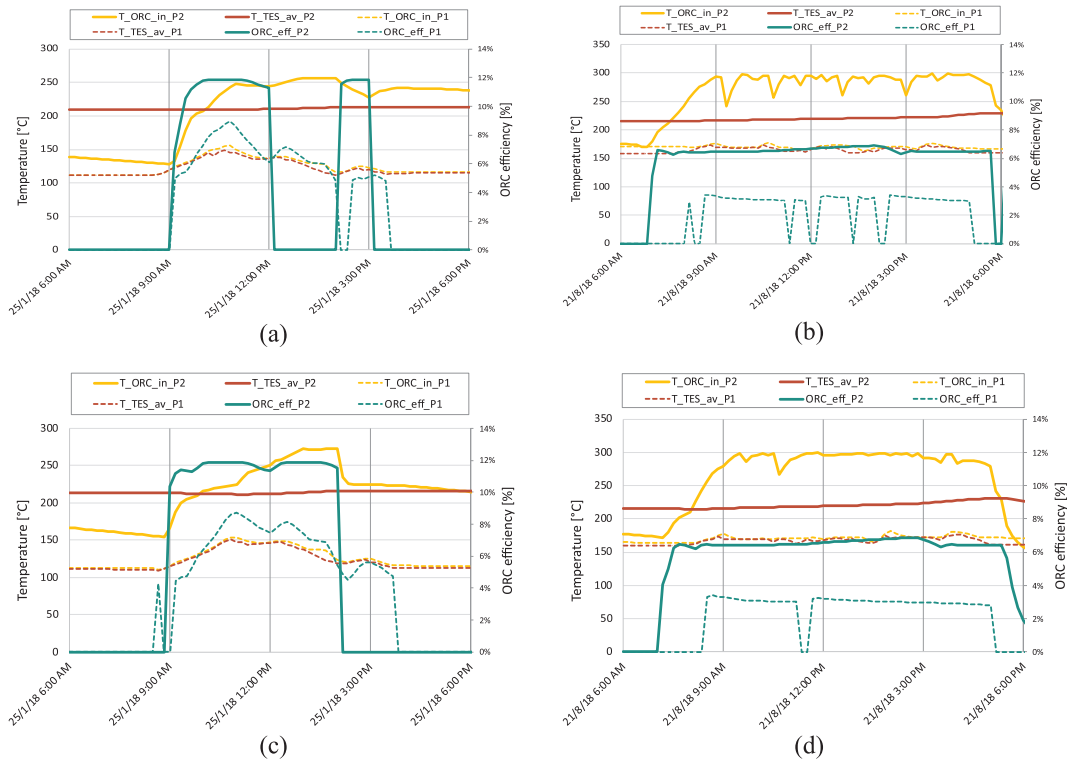

Fig. 7. Daily trend of ORC electric efficiency with temperatures for Plant 1 and Plant 2 in (a) winter in Napoli, (b) summer in Napoli, (c) winter in Messina, (d) summer in Messina.

systems have different thermal energy storage technologies integrated with different configurations and operational strategies. In particular the effect of the TES operating temperature is here discussed. Fig. 7a-d shows the daily trend of ORC electric efficiency together with the oil inlet temperature at the ORC evaporator and the average temperature of the storage tank of both plants for the typical winter and summer days in Napoli and Messina. Because of the lower concentration ratio of the CPC compared to the LFR, the inlet oil temperatures at the ORC unit and those of the storage tank are significantly lower in case of Plant 1. In Napoli, as anticipated, also during the winter day, the collected energy from the CPC solar field allows to achieve adequate temperatures at the HTT to run the ORC unit almost continuously in the period 9 am − 3 pm. On the contrary, despite the higher solar radiation during the summer day, Plant 1 has a tendency to frequent interruptions, because of its operation strategy. Indeed the limited operating temperature range of the HTT (see Table 1) and the higher condensing temperature in summer do not allow to maintain the minimum design temperature difference between the evaporator and the condenser of the ORC at 50 °C for prolonged periods (especially due to the limited capacity of the absorption chiller for the heat available). In case of Plant 2, the collected thermal energy allows to achieve the nominal ORC inlet temperature in short time also during the winter day. However, it is not enough to charge the PCM up to its melting temperature and then most part of this energy is lost. Moreover, because of the low input thermal power to the solar field after noon, the ORC unit is switched off also during the day as previously discussed. During the summer day, instead, the collected thermal energy from the LFR is so high that it allows to achieve high oil temperatures at the inlet of the ORC and melt the PCM at the same time, as reported in Fig. 7b. Similar trends occur in Messina also. However, in Messina Plant 1 exhibits limited shutdown during the summer day and Plant 2 runs without interruptions in the period 9 am − 2 pm also during the typical winter day, because of the different profile of solar irradiance.

6. Conclusions

In this work two different innovative solar ORC plants for trigeneration applications in the residential sector have been investigated by means of a numerical analysis in TRNSYS. Specific subroutines have been developed in Matlab by the authors to model the main components in detail.

The dynamic performance of the considered systems has been evaluated with respect to two Italian locations representative of the Mediterranean climate distinguished by different radiation conditions. The comparison, that for the first time regards a complete in-depth analysis of two solar ORC trigeneration systems powered by different CSP technologies, has brought to draw some interesting conclusions about the potential of different trigenerative systems and CSP technologies in particular.

In general, the investigation has revealed the great influence of solar radiation on the effectiveness of such systems even for locations at similar latitudes. In particular, the main findings are summarized below:

- the LFR-ORC system shows an energy performance very sensitive to location. In Messina, indeed, the electrical and thermal energy production of the ORC unit when powered by LFR is about 19% greater than in Napoli. Furthermore, this plant exhibits significant changes in energy production during the year and therefore seasonality has a considerable impact on this trend;
- the CPC-ORC is able to guarantee an electric and thermal energy output more constant throughout the year and less dependent on the quality of radiation, even if energy production is lower than LFR-ORC plant for both locations. Moreover, in summer, when the condensing temperatures are higher due to the absorption chiller, the electrical efficiency of the CPC-ORC is considerably limited;
- the LFR-ORC plant is able to achieve higher electric energy

production despite the lower size of the ORC. Furthermore, in summer the LFR technology achieves higher conversion efficiencies that allow to obtain a significant thermal output from the ORC unit. As a consequence, in case of high DNI, LFR technology performs much better than CPC and thus results especially suitable for solar cooling applications;
- the higher operation temperatures of the latent heat TES of the considered LFR-ORC plant compared to the sensible heat TES of the CPC-ORC plant allow higher electric efficiency of the ORC, but at the same cause higher thermal losses in winter time if the melting temperature of the PCM is not reached. As a consequence, a proper management of the latent heat TES is recommended to increase the overall efficiency of solar plants using such kind of thermal energy storage technology.

In conclusion, this study has highlighted the importance of proper design and technology selection with different radiation conditions, thus serving as a general guide for the adoption of similar technologies for trigeneration purposes at residential level in areas with a Mediterranean climate.

Acknowledgements

Appendix A. Supplementary material

Supplementary data to this article can be found online at https://doi.org/10.1016/j.apenergy.2019.03.066.

References

[1] Pietzcker RC, Stetter D, Manger S, Luderer G. Using the sun to decarbonize the power sector: The economic potential of photovoltaics and concentrating solar power. Appl Energy 2014;135:704–20. https://doi.org/10.1016/j.apenergy.2014.08.011.

[2] IEA. Technology roadmap solar thermal electricity; 2014. https://doi.org/10.1007/SpringerReference_7300.

[3] Watkins P, McKendry P. Assessment of waste derived gases as a renewable energy source – Part 2. Sustain Energy Technol Assess 2015;10:114–24. https://doi.org/10.1016/j.seta.2015.03.004.

[4] Barlev D, Vidu R, Stroeve P. Innovation in concentrated solar power. Sol Energy Mater Sol Cells 2011;95:2703–25. https://doi.org/10.1016/j.solmat.2011.05.020.

[5] Jebasingh VK, Herbert GMMJ. A review of solar parabolic trough collector. Renew Sustain Energy Rev 2016;54:1085–91. https://doi.org/10.1016/j.rser.2015.10.043.

[6] Zhu G, Wendelin T, Wagner MJ, Kutscher C. History, current state, and future of linear Fresnel concentrating solar collectors. Sol Energy 2014;103:639–52. https://doi.org/10.1016/j.solener.2013.05.021.

[7] Abbas R, Muñoz J, Martínez-Val JM. Steady-state thermal analysis of an innovative receiver for linear Fresnel reflectors. Appl Energy 2012;92:503–15. https://doi.org/10.1016/j.apenergy.2011.11.070.

[8] Santos-González I, García-Valladares O, Ortega N, Gómez VH. Numerical modeling and experimental analysis of the thermal performance of a Compound Parabolic Concentrator. Appl Therm Eng 2017;114:1152–60. https://doi.org/10.1016/j.applthermaleng.2016.10.100.

[9] Carrilho da Graça G, Augusto A, Lerer MM. Solar powered net zero energy houses for southern Europe: Feasibility study. Sol Energy 2012;86:634–46. https://doi.org/10.1016/j.solener.2011.11.008.

[10] Quoilin S, Van Den Broek M, Declaye S, Dewallef P, Lemort V. Techno-economic survey of organic rankine cycle (ORC) systems. Renew Sustain Energy Rev 2013;22:168–86. https://doi.org/10.1016/j.rser.2013.01.028.

[11] Desai NB, Bandyopadhyay S. Thermo-economic analysis and selection of working fluid for solar organic Rankine cycle. Appl Therm Eng 2016;95:471–81. https://doi.org/10.1016/j.applthermaleng.2015.11.018.

[12] Quoilin S, Orosz M, Hemond H, Lemort V. Performance and design optimization of

a low-cost solar organic Rankine cycle for remote power generation. Sol Energy 2011;85:955–66. https://doi.org/10.1016/j.solener.2011.02.010.

[13] Taccani R, Obi JB, De Lucia M, Micheli D, Toniato G. Development and experimental characterization of a small scale solar powered organic rankine cycle (ORC). Energy Procedia 2016;101:504–11. https://doi.org/10.1016/j.egypro.2016.11.064.

[14] Bouvier JL, Michaux G, Salagnac P, Kientz T, Rochier D. Experimental study of a micro combined heat and power system with a solar parabolic trough collector coupled to a steam Rankine cycle expander. Sol Energy 2016;134:180–92. https://doi.org/10.1016/j.solener.2016.04.028.

[15] Ghasemi H, Sheu E, Tizzanini A, Paci M, Mitsos A. Hybrid solar-geothermal power generation: Optimal retrofitting. Appl Energy 2014;131:158–70. https://doi.org/10.1016/j.apenergy.2014.06.010.

[16] Freeman J, Hellgardt K, Markides CN. An assessment of solar-powered organic Rankine cycle systems for combined heating and power in UK domestic applications. Appl Energy 2015;138:605–20. https://doi.org/10.1016/j.apenergy.2014.10.035.

[17] Ramos A, Chatzopoulou MA, Freeman J, Markides CN. Optimisation of a high-efficiency solar-driven organic Rankine cycle for applications in the built environment. Appl Energy 2018. https://doi.org/10.1016/j.apenergy.2018.06.059.

[18] Freeman J, Hellgardt K, Markides CN. Working fluid selection and electrical performance optimisation of a domestic solar-ORC combined heat and power system for year-round operation in the UK. Appl Energy 2017;186:291–303. https://doi.org/10.1016/j.apenergy.2016.04.041.

[19] Manfrida G, Secchi R, Stańczyk K. Modelling and simulation of phase change material latent heat storages applied to a solar-powered Organic Rankine Cycle. Appl Energy 2016;179:378–88. https://doi.org/10.1016/j.apenergy.2016.06.135.

[20] Esen M, Ayhan T. Development of a model compatible with solar assisted cylindrical energy storage tank and variation of stored energy with time for different phase change materials. Energy Convers Manag 1996. https://doi.org/10.1016/0196-8904(96)00035-0.

[21] Esen M, Durmuş A, Durmuş A. Geometric design of solar-aided latent heat store depending on various parameters and phase change materials. Sol Energy 1998. https://doi.org/10.1016/S0038-092X(97)00104-7.

[22] Esen M. Thermal performance of a solar-aided latent heat store used for space heating by heat pump. Sol Energy 2000. https://doi.org/10.1016/S0038-092X(00)00015-3.

[23] Boyaghchi FA, Heidarnejad P. Thermoeconomic assessment and multi objective optimization of a solar micro CCHP based on Organic Rankine Cycle for domestic application. Energy Convers Manag 2015;97:224–34. https://doi.org/10.1016/j.enconman.2015.03.036.

[24] Karellas S, Braimakis K. Energy-exergy analysis and economic investigation of a cogeneration and trigeneration ORC-VCC hybrid system utilizing biomass fuel and solar power. Energy Convers Manag 2016;107:103–13. https://doi.org/10.1016/j.enconman.2015.06.080.

[25] Cioccolanti L, Tascioni R, Bocci E, Villarini M. Parametric analysis of a solar Organic Rankine Cycle trigeneration system for residential applications. Energy

Convers Manag 2018;163:407–19. https://doi.org/10.1016/J.ENCONMAN.2018.02.043.

[26] Innova-Microsolar; n.d.

[27] Ahlgren B, Tian Z, Perers B, Dragsted J, Johansson E, Lundberg K, et al. A simplified model for linear correlation between annual yield and DNI for parabolic trough collectors. Energy Convers Manag 2018;174:295–308. https://doi.org/10.1016/J.ENCONMAN.2018.08.008.

[28] Mohammadi K, Goudarzi N. Association of direct normal irradiance with El Niño Southern Oscillation and its consequence on concentrated solar power production in the US Southwest. Appl Energy 2018;212:1126–37. https://doi.org/10.1016/j.apenergy.2017.12.102.

[29] Kloben; n.d.

[30] Yazaki Energ Systems, Inc.; n.d.

[31] Therminol® 62 Heat Transfer Fluid; n.d. http://www.therminol.com/products/Therminol-62 [accessed August 28, 2017].

[32] Elianto S.R.L – Home; n.d.

[33] Enogia SAS. Enogia; n.d. http://www.enogia.com/ [accessed May 25, 2018].

[34] 3M. Novec™ 649; n.d. https://www.3m.com/3M/en_US/company-us/all-3m-products/~/3M-Novec-649-Engineered-Fluid/?N=5002385+3290667401&rt=rud [accessed May 25, 2018].

[35] Thermacore. Aavid Thermacore; n.d. https://www.thermacore.com/ [accessed May 25, 2018].

[36] Maldonado J, Fullana-Puig M, Martín M, Solé A, Fernández Á, de Gracia A, et al. Phase change material selection for thermal energy storage at high temperature range between 210 °C and 270 °C. Energies 2018;11:861. https://doi.org/10.3390/en11040861.

[37] Serrano-López R, Fradera J, Cuesta-López S. Molten salts database for energy applications. Chem Eng Process 2013. https://doi.org/10.1016/j.cep.2013.07.008.

[38] S.TRA.TE.G.I.E. S.TRA.TE.G.I.E.; n.d. http://www.strategiesrl.com/ [accessed May 25, 2018].

[39] TRNSYS – Transient System Simulation Tool; n.d. http://www.trnsys.com/ [accessed August 28, 2017].

[40] Matlab Mathworks; n.d. https://www.mathworks.com/products/matlab.html [accessed August 28, 2017].

[41] Gantenbein P, Jaenig D, Kerskes H, Van Essen M. Final report of Subtask B "Chemical and Sorption Storage"; The overview. A Report of IEA Solar Heating and Cooling programme -Task 32 Advanced storage concepts for solar and low energy buildings Report B7 of Subtask B. 2008.

[42] Cioccolanti L, Tascioni R, Arteconi A. Mathematical modelling of operation modes and performance evaluation of an innovative small-scale concentrated solar organic Rankine cycle plant. Appl Energy 2018;221:464–76. https://doi.org/10.1016/j.apenergy.2018.03.189.

[43] Calise F, d'Accadia MD, Vicidomini M, Scarpellino M. Design and simulation of a prototype of a small-scale solar CHP system based on evacuated flat-plate solar collectors and Organic Rankine Cycle. Energy Convers Manag 2015;90:347–63. https://doi.org/10.1016/j.enconman.2014.11.014.